THE JOURNAL OF BIOLOGICAL CHEMISTRY VOL. 287, NO. 32, pp. 26921–26931, August 3, 2012

Charge Compensation Mechanism of a Na^+-coupled, Secondary Active Glutamate Transporter*[S]

Received for publication, March 19, 2012, and in revised form, June 14, 2012 Published, JBC Papers in Press, June 15, 2012, DOI 10.1074/jbc.M112.364059

Christof Grewer[‡1], Zhou Zhang[§], Juddy Mwaura[‡], Thomas Albers[‡], Alexander Schwartz[‡], and Armanda Gameiro[‡]

From the [‡]Department of Chemistry Binghamton University, Binghamton, New York 13902 and the [§]College of Life and Environment Sciences, Shanghai Normal University 100, Guilin Road, Shanghai 200234, China

Background: Reorientation of the binding sites of the glutamate transporter requires K^+ translocation.
Results: Single turnover K^+ translocation is associated with negative transmembrane charge movement.
Conclusion: The empty glutamate transporter carries an apparent charge of −1.23, overcompensating for the positive charge of the translocated K^+ ion.
Significance: Charge compensation may be a general strategy of Na^+-dependent transporters to overcome electrostatic barriers of charge transport.

Forward glutamate transport by the excitatory amino acid carrier EAAC1 is coupled to the inward movement of three Na^+ and one proton and the subsequent outward movement of one K^+ in a separate step. Based on indirect evidence, it was speculated that the cation binding sites bear a negative charge. However, little is known about the electrostatics of the transport process. Valences calculated using the Poisson-Boltzmann equation indicate that negative charge is transferred across the membrane when only one cation is bound. Consistently, transient currents were observed in response to voltage jumps when K^+ was the only cation on both sides of the membrane. Furthermore, rapid extracellular K^+ application to EAAC1 under single turnover conditions (K^+ inside) resulted in outward transient current. We propose a charge compensation mechanism, in which the C-terminal transport domain bears an overall negative charge of −1.23. Charge compensation, together with distribution of charge movement over many steps in the transport cycle, as well as defocusing of the membrane electric field, may be combined strategies used by Na^+-coupled transporters to avoid prohibitive activation barriers for charge translocation.

Glutamate transport by the members of the SLC1 family (1, 2), as well as secondary active transport by other solute carriers (3), is thought to occur through an alternating access mechanism (4). Such mechanisms assume that the transporter cycles through at least two discrete conformational states, one of them allowing access of substrate to its binding site from the extracellular side and the other one allowing access from the cytoplasm. Glutamate and 3 Na^+ ions, when bound to the transporter at the same time, initiate the conformational change(s) associated with alternating accessibility. Based on recent crystallographic and computational evidence, it was hypothesized that alternating accessibility is mediated by sequential movement of an external gate (reentrant loop 2 (5–7)) and an internal gate (reentrant loop 1 (2, 8)).

In addition to the opening and closing of gates, glutamate transport is thought to be associated with large scale, rigid body conformational changes (9), one of them being the movement of the C-terminal transport domain that leads to the translocation of glutamate along the bilayer normal (1, 2). This movement has been described in terms of a hydrophobic interaction mechanism, in which the trimerization domain provides an unstructured, hydrophobic surface, along which the transport domain can move inward and outward (2). Due to the large number of potentially charged residues that are moved in the transport process, it is likely that in addition to the hydrophobic effect, electrostatics play an important role. Because the movement of 3 Na^+ ions across the hydrophobic barrier of the membrane is expected to be unfavorable, it has been suggested that the positive charge of the cations is at least partially compensated for by negative charge of the binding site(s) (10–12). Consistent with this suggestion, several negatively charged amino acid residues, which are highly conserved within the SLC1 family and sensitive to mutation, are located in the C-terminal transport domain (13–16).

K^+ also initiates alternating accessibility in a step separable from Na^+/glutamate movement (K^+ countertransport (10, 17, 18)). Based on indirect evidence from the voltage dependence of steady-state glutamate-induced transport currents (10, 19), as well as measurements on fluorescently labeled transporters (11), it was speculated that the K^+ relocation step(s) is associated with net negative charge movement, despite the positive charge of the transported K^+ ion. However, no direct experimental evidence for the voltage dependence of the K^+ relocation step(s) has been obtained.

In this work, we have used a combination of experimental and computational methods to test the charge compensation hypothesis. Our results show that conformational changes associated with K^+-K^+ exchange proceed in at least two electrogenic steps with net negative charge movement. Consistently, computations of electrostatic energies demonstrate negative valence of the relocation step. K^+ binding depends on

* This work was supported, in whole or in part, by National Institutes of Health Grant 2R01NS049335-06A1 (to C. G.). This work was also supported by Binational Science Foundation Grant 2007051 (to C. G. and B. I. Kanner).
[S] This article contains supplemental Methods, Table 1, and Figs. 1–9.
[1] To whom correspondence should be addressed: Dept. of Chemistry, Binghamton University, 4400 Vestal Pkwy. E., Binghamton, NY 13902. Tel.: 607-777-3250; Fax: 607-777-4478; E-mail: cgrewer@binghamton.edu.

voltage only to a small extent. The results are consistent with a multistep charge compensation mechanism, in which fast cation binding precedes electrogenic cation exchange through an overall negatively charged transport domain.

EXPERIMENTAL PROCEDURES

Cell Culture, Transfection, Whole-cell Current Recording, and Site-directed Mutagenesis—HEK293 cells (American Type Culture Collection number CRL 1573) were cultured as described previously (10, 12). The cell cultures were transiently transfected with wild-type or mutant EAAC1 cDNA inserted into a modified pBK-CMV expression plasmid (10) by using FuGene HD transfection reagent according to the protocol supplied by the manufacturer (Roche Applied Science). One day after transfection, the cells were used for electrophysiological measurements. Glutamate-induced EAAC1 currents were measured in the whole-cell current recording configuration. Whole-cell currents were recorded with an EPC7 patch clamp amplifier (ALA Scientific, Westbury, NY) under voltage clamp conditions. The resistance of the recording electrode was 2–3 megaohms, as described previously (12).

In the whole-cell recordings performed at steady state, series resistance was not compensated for because of the small whole-cell currents carried by EAAC1. However, series resistance compensation of 60–80% as well as whole-cell capacitance cancellation were used in the whole-cell recording experiments involving step changes of the membrane potential, in order to accelerate the capacitive charging of the membrane in response to the voltage jump. Typical time constants for membrane charging under these conditions were 200–250 μs (20).

Ionic Conditions for K^+ Exchange Experiments—K^+/Cs^+ exchange was established by using symmetrical $[K^+]$ on both sides of the membrane (140 mM) in the absence of Na^+ and glutamate. The composition of the solutions was as follows: 140 mM K/CsMes, 2 mM $Mg(gluconate)_2$, 2 mM $Ca(gluconate)_2$, 10 mM HEPES, pH 7.3 (extracellular), 140 mM K/CsMes, 2 mM $Mg(gluconate)_2$, 5 mM EGTA, 10 mM HEPES, pH 7.3 (intracellular). To obtain the specific component of the currents, we subtracted nonspecific currents in the presence of the competitive inhibitor DL-*threo*-β-benzyloxyaspartate (TBOA)[2] (21). TBOA does not bind to EAAC1 in the absence of Na^+ and may bind, but only weakly, in the presence of extracellular K^+. Therefore, TBOA binding was promoted by including a small amount of Na^+ (2 mM in the presence of extracellular K^+ and 5 mM in the presence of extracellular NMG^+) in the TBOA-containing solution, as described previously (22). This small amount of Na^+ did not elicit nonspecific currents. Under these ionic conditions, 200 μM TBOA is a supersaturating concentration (about 100-fold K_m), so the TBOA binding site should be saturated at all voltages. The K_m for TBOA under these conditions has been experimentally determined previously (22).

Ionic Conditions for Na^+/Glutamate Exchange Experiments—Glutamate/Na^+ exchange was established by using symmetrical $[Na^+] = 140$ mM and [glutamate] = 10 mM on both sides of the membrane. Under these conditions, the internal and external binding sites for Na^+ and glutamate should be saturated, based on results from previous studies (12, 22). The composition of the solutions was as follows: 140 mM NaMes, 2 mM $Mg(gluconate)_2$, 2 mM $Ca(gluconate)_2$, 10 mM HEPES, 10 mM glutamate, pH 7.3 (extracellular), 140 mM NaMes, 2 mM $Mg(gluconate)_2$, 5 mM EGTA, 10 mM HEPES, 10 mM glutamate, pH 7.3 (intracellular). Ionic conditions for forward and reverse transport were as published previously (10).

For charge-voltage relationships, we used the Boltzmann equation to fit the experimental data.

$$Q = \frac{Q_{max}}{1 + \exp\left(\frac{-z_Q F(V - V_{1/2})}{RT}\right)} + Q_{offset} \quad \text{(Eq. 1)}$$

Here, Q_{max} is the maximum charge movement, and Q_{offset} is the holding potential-dependent offset of the charge movement, $V_{1/2}$ is the midpoint potential, and F is the Faraday constant. R and T have their usual meaning, and z_Q is the valence of the charge movement, which is obtained from the fit.

Computation of the Valence of the Transport Domain—We have used the Adaptive Poisson-Boltzmann Solver (APBS) (23), together with the APBSmem Java routines (24) for the calculation of electrostatic energies of the glutamate transporter embedded into an implicit membrane. In the presence of an internal membrane potential, V, the following modified version of the linearized Poisson-Boltzmann equation is used, according to the formalism first introduced by Roux (25).

$$-\nabla(\epsilon(\vec{r})\nabla\phi(\vec{r})) + \kappa^2(\vec{r})\phi(\vec{r}) = \frac{e4\pi}{k_bT}\left(\rho(\vec{r}) + \frac{\kappa^2 V}{4\pi} f(\vec{r})\right) \quad \text{(Eq. 2)}$$

Here, ϵ is the dielectric constant, which depends on the spatial coordinate, $\phi = e\Phi/k_bT$, where Φ is the electrostatic potential, e is the elementary charge, T is the temperature, and k_b is the Boltzmann constant. κ is the Debye-Hückel screening constant, and ρ is the charge density. $f(r)$ is the Heaviside step function, which is set to 1 in the intracellular solution and is 0 in the membrane, protein, and extracellular solution. Details of the method can be found in Ref. 24.

The total electrostatic energy, E, is then computed by summing up over the product of the local charge and the potential (26),

$$E = \int \phi(\vec{r})\rho(\vec{r})\mathrm{d}V \quad \text{(Eq. 3)}$$

where $\mathrm{d}V$ is the volume element. To compute the valence, membrane potentials of varying magnitude, V, are applied to the internal side of the membrane, and the difference in total electrostatic energy, ΔE, for two protein configurations (*e.g.* inward and outward facing conformations) is calculated. When plotting ΔE *versus* the membrane potential, the valence is obtained from the slope (27). Energy contributions that do not come from movement of protein charges have been subtracted in this approach, after calculating the electrostatic energy in the

[2] The abbreviations used are: TBOA, DL-*threo*-β-benzyloxyaspartate; APBS, Adaptive Poisson-Boltzmann Solver; PB, Poisson-Boltzmann.

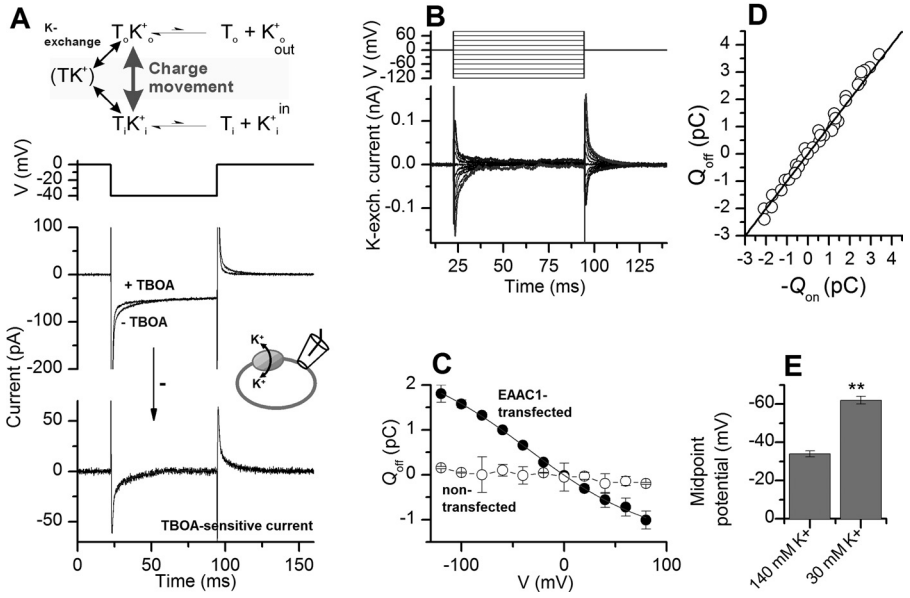

FIGURE 1. **K^+-induced relocation is associated with charge movement.** *A*, voltage jump procedure used to isolate EAAC1-specific transient currents associated with K^+ exchange. The *middle panel* shows original current traces measured in response to a voltage jump (*top panel*) in the absence (−*TBOA*) and presence (+*TBOA*) of 200 μM blocker TBOA (21). The *bottom panel* shows the EAAC1-specific, TBOA-sensitive component obtained by subtraction of the +TBOA from the −TBOA trace. *B* and *C*, voltage dependence of TBOA-sensitive K^+ exchange currents (*middle panel*) and charge movement (Q_{off} (●), off-response of slow phase obtained by calculating the time integral of the current). The *solid line* represents a fit to a Boltzmann equation with an apparent valence of 0.41. ○, control experiments from non-transfected cells. *D*, the charge movement of the off-response (Q_{off}) scales with that of the on-response (Q_{on}). The *solid line* has a slope of 1. *E*, [K^+] dependence of the midpoint potential. *Error bars*, S.D.

absence of protein charges. The details of the APBSmem setup are described in the supplemental Methods.

The APBSmem approach was validated by using a model system, in which a Na^+ ion was moved from the water phase into a membrane of 30 Å thickness at a distance of 10 Å below the membrane surface. As expected, the valence of this transition was 0.32.

RESULTS

K^+-induced Relocation of the Transporter Is Associated with Charge Movement—We first tested whether K^+-dependent reaction steps of EAAC1 are electrogenic, by locking the transporter in the K^+ exchange mode (Fig. 1*A*, *top*). Step changes in the membrane potential under K^+ exchange conditions (Fig. 1*A*) induced transient, TBOA-sensitive currents, which decayed with two-exponential components (Fig. 1*A*). Little voltage-induced charge movement was seen under the same conditions in non-transfected cells (Fig. 1*C*). As expected, the charge scales linearly with the expression level ($n = 12$ cells; supplemental Fig. 1) and is virtually eliminated at low extracellular [K^+] (5 mM; supplemental Fig. 3). The transient currents were capacitive in nature (Fig. 1, *A* and *D*). The charge movement was voltage-dependent with an apparent valence of 0.41 (supplemental Methods and supplemental Fig. 1, *B* and C) and with a [K^+]-dependent midpoint potential (Fig. 1*E*). Together, these results suggest that voltage jumps result in a redistribution of the electrogenic K^+ exchange equilibrium. This redistribution consists of at least two steps, as indicated by the two exponential components of the transient current decay (supplemental Fig. 2). One component was fast in the microsecond range (average $\tau = 0.85 \pm 0.2$ ms, $n = 8$), and the other was about 15-fold slower (average $\tau = 13 \pm 3$ ms, $n = 8$).

Contribution of Electrostatics to Conformational Transitions—To test the hypothesis of electrogenic K^+-dependent relocation, we computed the valence of the K^+-loaded transporter, using the APBS routine (23), numerically solving the linearized Poisson-Boltzmann (PB) equation for various transporter/implicit membrane systems. The simulation setup is shown in Fig. 2*A*. The transporter structures were obtained by homology modeling of the EAAT3 sequence based on the GltPh (aspartate transporter from *Pyrococcus horikoshii*) template structures (Protein Data Bank codes 2NWX and 3KBC (2, 8)). In addition, we used a simplified model, in which only the conserved charged residues were modeled in the absence of protein but retained their correct orientations (Fig. 2*B*). A biasing potential (Fig. 2, *A*, C, and *D*) applied to the intracellular side (24) allows the determination of voltage drop within the transmembrane domain in the absence of intrinsic charges of the protein (25). As a first approximation, we neglected the dipole potential of the membrane. Fig. 2, *C* and *D*, shows isopotential planes for transporters, in which all subunits are outward facing (Fig. 2*C*) and in which one subunit is inward facing (Fig. 2*D*; assuming that the subunits transport glutamate independently (9, 28)). Transition to the inward facing configuration results in an altered distribution of isopotential planes, with the voltage drop shifted toward the intracellular direction (Fig. 2*E*). Clearly, such a shift in the interaction of the membrane electric field with the transporter must result in a voltage dependence of the conformational transition if the transmembrane domain of the transporter is charged. Interestingly, insertion of the transport protein into the membrane leads to a defocusing of the transmembrane electric field, as compared with the voltage drop for the membrane-only system in the absence of protein (Fig. 2*E*).

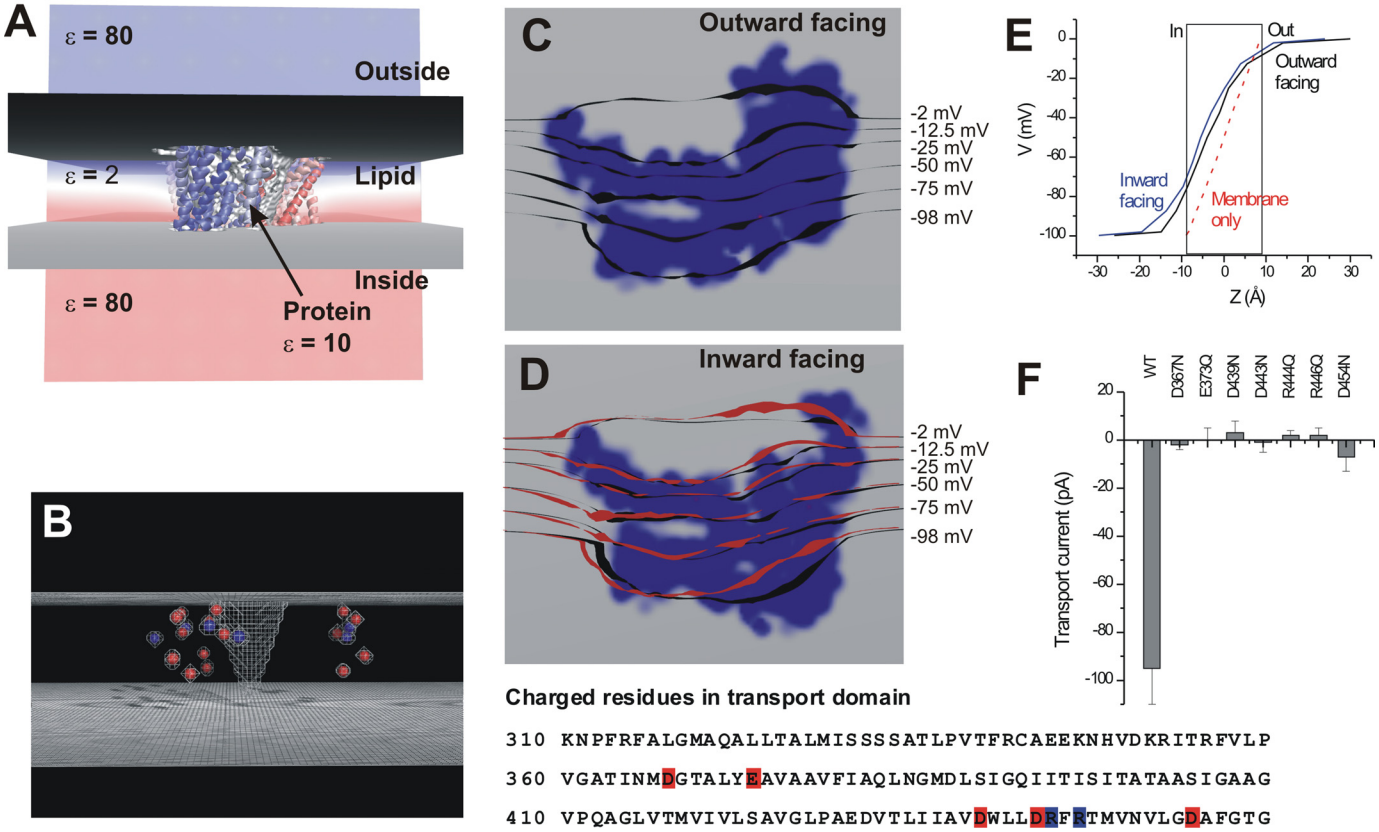

FIGURE 2. **Interaction of the transport domain with the transmembrane electric field.** *A*, setup of the EAAC1/implicit membrane system. The voltage is *color-coded* as follows: *blue*, 0 mV; *red*, −100 mV; *white*, −50 mV. *B*, a minimalistic charge/membrane/solvent system, in which only the seven conserved charged residues were modeled. *C* and *D*, isopotential planes for transporters with three outward facing subunits (*C*) and two outward facing and one inward facing subunit (*D*, *black*), calculated using the linearized PB equation (protein indicated in *blue*). The *red planes* show the superposition of isopotential planes from *C*. *E*, V_m as a function of the *z* direction (perpendicular to the membrane plane) for outward facing conformation (*black*), inward facing conformation (*blue*), and membrane only (20 Å wide; *red*). The potential was sampled at *x* and *y* coordinates at the center of the individual subunit (substrate binding site). *F*, average steady-state transport currents ($n > 3$) for EAAC1 with several conservative mutations (see sequence (*bottom*); forward transport mode, $V = 0$ mV). *Error bars*, S.D.

Several charged amino acid residues are conserved within the C-terminal transport domain of the glutamate transporter family, including five acidic amino acids and two potentially positively charged residues (Fig. 2, *sequence inset*). Conservative, charge-neutralizing mutation of all of these residues results in defects in glutamate transport (Fig. 2*F*). This result indicates that these potentially charged residues may be important for electrostatic charge compensation. Valences for the outward-to-inward facing transition for all mutant transporters, as calculated through PB analysis, are listed in supplemental Table 1. As expected, charge-neutralizing mutations at positions that move the largest distance within the membrane electric field (Asp-443, Arg-444, and Arg-446), show the largest deviations from the EAAC1(WT) valence.

The C-terminal Transport Domain of the Glutamate Transporter Carries Net Negative Charge—Next, we computed the theoretical valence associated with several transitions in the transport cycle, by calculating the difference in total electrostatic energy, ΔE, of the transporter/membrane systems before and after the structural change as a function of the membrane potential, V_m (Fig. 3, *A* and *B*) (23). The slope of the ΔE *versus* V_m relationship is representative of the valence of the charge movement (24, 27). We first investigated what is believed to be the major structural change associated with glutamate transport from the outward facing to the inward facing conformation (1, 2) (Fig. 3*C*). The valence of the charge movement was negative in the absence of any bound cations ($z = -1.23$) or in the presence of only one bound cation (Cs^+, $z = -0.59$, or K^+, Fig. 3*A*, *top*), with negative potential stabilizing the outward facing configuration. The valence did not depend strongly on the exact positioning of the cation (positioned in the GltPh Na1 site or in the substrate binding site, as suggested in Ref. 29). The transporter became almost neutralized with two Na^+ ions bound. In the presence of an additional third Na^+ ion and a proton (protonation of Glu-373 (30)) and in the fully loaded configuration (with glutamate), the valence of the charge movement reverted to a positive sign ($z = +0.15$; Fig. 3, *A* and *B*). This result suggests that the negative charge of the transporter binding sites and the bound glutamate partially compensates for the positive charges of the three bound Na^+ ions and the proton, consistent with several reports showing inward charge movement of Na^+/glutamate translocation (12, 19, 20). Consequently, transient currents were observed when the transporter was subjected to voltage jumps in the Na^+/glutamate exchange mode (Fig. 3*D*). In the exchange mode, charge movement is caused mainly by the actual conformational transitions of the transporter but to a lesser extent by cation/substrate binding or unbinding.

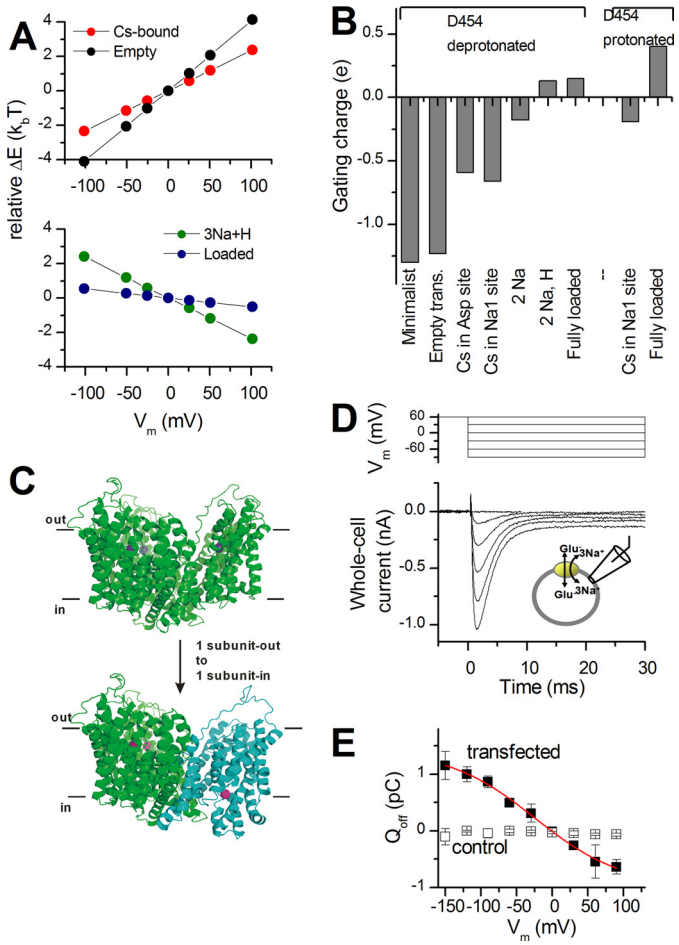

FIGURE 3. **The binding sites of the empty transporter carry negative charge.** *A*, principle of PB computations of the valence of outward facing-to-inward facing transition of EAAC1 of the empty transporter (*black*) with Cs^+ bound (*red*), three Na^+ and H^+ bound (*green*), and fully loaded (*blue*). *B*, computed valence for the outward facing-to-inward facing transition of EAAC1 loaded with different numbers/types of cations and with and without substrate. *C*, illustration of the starting and end state of the system (bound Cs^+ is indicated in *purple*). *Green*, outward facing; *turquoise*, inward facing. *D*, TBOA-sensitive transient currents in response to the voltage jump protocol (*top*) in the Na^+/glutamate exchange mode (*inset*). The external solution contained 140 mM Na^+ and 1 mM glutamate, and the internal solution contained 120 mM Na^+ and 10 mM glutamate. *E*, voltage dependence of the charge movement in EAAC1-expressing (*black squares*) and non-transfected (*open squares*) cells. The *red line* represents a fit to the Boltzmann equation with an apparent valence of 0.43. *Error bars*, S.D.

The apparent valence of the charge movement was 0.43 ± 0.1. This valence is larger than the theoretical computed value shown above for the fully loaded transporter (+0.15). Therefore, it is possible that the negative charge of the binding sites is overestimated because not all acidic side chains are deprotonated. Although previous pK_a computations suggested that Asp-454 is deprotonated at pH 7.4 (31), we computed the valence with a protonated Asp-454. A *z* of +0.40 was found for the fully loaded transporter. This value agrees well with the experimentally observed valence (0.43; Fig. 3*E*), raising the possibility that Asp-454 is protonated in the fully loaded transporter, consistent with its location deeply buried in the interior of the protein.

Charge Movement Is Slowed by Cs^+ Substitution—If steps associated with K^+ binding and/or relocation are electrogenic, they should be sensitive to the nature of the monovalent cation. It is known for other glutamate transporter subtypes that Cs^+ can substitute for K^+, but Cs^+ is transported at a lower rate than K^+ (32, 33), although transport was also increased by Cs^+ in one report (34). Consistent with this hypothesis, forward transport currents (Fig. 4, *A–C*) as well as reverse transport (Fig. 4, *B* and *D*) currents in EAAC1 were reduced about 2–2.5-fold when Cs^+ was used instead of K^+ as the cation on the *trans* side of the membrane. Therefore, we used Cs^+ substitution on both sides of the membrane (Fig. 4*E*, *inset*) to obtain further information on the voltage jump-induced charge movements. As shown in Fig. 4*E*, transient current relaxations in the sole presence of Cs^+ in response to voltage jumps from −90 to 0 mV transmembrane potentials were biphasic, as in K^+, but displayed smaller peak amplitudes and slower relaxation kinetics. Reduction of the peak current in Cs^+, which resulted in a lower signal/noise ratio (Fig. 4*E*), is expected because the same charge is displaced over a longer time window. The fast phase of the current decay was slowed about 4-fold with a relaxation time constant of 3.3 ± 1.5 ms (n = 6), whereas the slow phase was about 1.6-fold slower with a time constant of 21 ± 4 ms (averages shown in Fig. 4*F*). Relaxation rate constants in both Cs^+ and K^+ were smaller than the rate constants associated with equilibration of the Na^+/glutamate translocation step(s) (glutamate exchange mode), as shown in Fig. 4*E*. This result is consistent with previous suggestions that K^+ relocation, but not Na^+/glutamate translocation, limits the overall turnover rate of the glutamate transporter subtype EAAC1 (10).

Extracellular K^+ Binding Is Electrically Silent—A glutamate transporter with the mutation E373Q was previously shown to be defective in K^+-dependent relocation (30, 35) while still being able to bind extracellular potassium and catalyze Na^+-dependent glutamate translocation (30). As expected, step changes of the membrane potential to EAAC1(E373Q) in the Na^+/glutamate exchange mode resulted in large transient transport currents (Q = 320 ± 15 femtocoulombs, n = 5; Fig. 5, *A* and *C*). In contrast, charge movement was virtually eliminated in the K^+ exchange mode (Q = 22 ± 3 femtocoulombs, n = 5; Fig. 5, *B* and *C*). This result suggests that the voltage-dependent charge movement observed in the K^+ exchange mode is caused mainly by K^+ translocation but not by K^+ binding to its binding site. Consistently, the apparent affinity of the transporter for extracellular K^+ or Cs^+ in the reverse transport mode was virtually independent of the transmembrane potential (supplemental Fig. 4, *A–C*).

We next performed PB calculations for K^+ binding to three potential binding sites at positions suggested by previous mutagenesis experiments (14, 29, 35). The valence associated with movement of K^+ into the substrate binding site (a binding site suggested in Ref. 29) is +0.106 (Fig. 5*D*). In contrast, the Asp-454 cation binding site (Na1 site in GltPh) is more deeply buried in the membrane, resulting in a valence of K^+ binding of +0.34 (Fig. 5, *D–F*). However, direct accessibility of this site to a cation is unlikely because no aqueous pathway exists for an ion to move into this site (31). To obtain an apo-like configuration for the PB analysis, we performed molecular dynamics simulations in the absence of any bound ions/substrates (supplemental Fig. 5). In agreement with previous reports (6, 7, 31), reentrant loop 2 opens after several ns while, simultaneously,

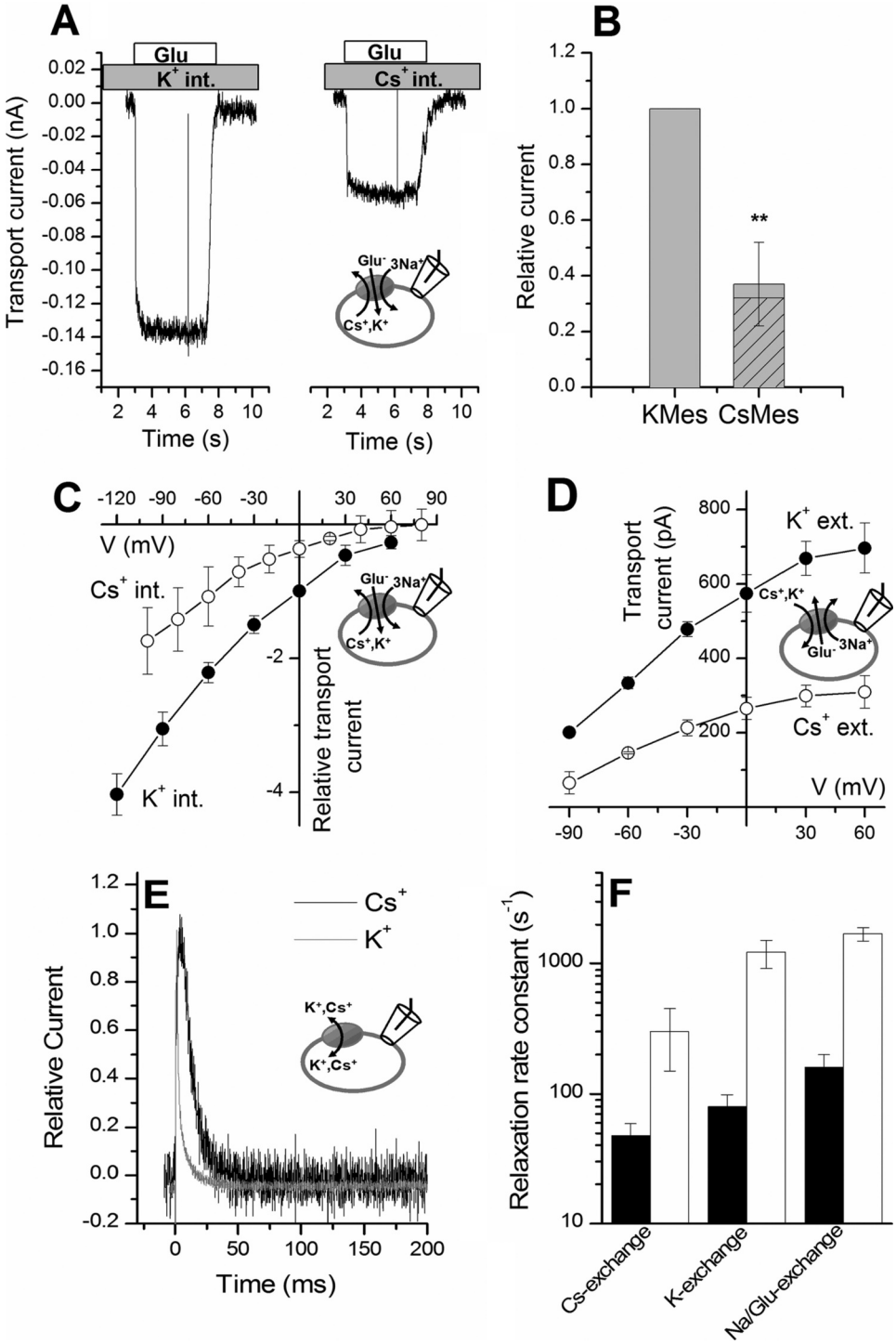

FIGURE 4. **Cation dependence of the voltage-dependent relocation step(s) of the transporter.** *A*, original traces for transport currents induced by 100 μM glutamate in the presence of intracellular KMes (*left*) and CsMes (*right*). *c* (cation) = 140 mM, V_m = 0 mV. The extracellular solution contained 140 mM NaMes. The data are from the same cell. The intracellular solution was changed from K^+ to Cs^+ through diffusion, by backfilling a KMes-dipped pipette with CsMes solution. *B*, statistical analysis of data from seven different cells. The *hashed bars* represent data from the same cells as the K^+ control. *C*, current-voltage relationship of inward transport currents with intracellular KMes (●) and CsMes (○). *D*, current-voltage relationship of outward transport currents in the presence of 140 mM KMes (●) and CsMes (○). The intracellular solution contained 10 mM glutamate and 140 mM NaMes. The EAAC1-specific current component was isolated by determining its sensitivity to 200 μM extracellular TBOA (a saturating concentration) in the presence of 2 mM Na^+. *E*, off-response recorded after stepping the membrane potential from −90 mV back to 0 mV in the Cs^+ exchange (*black trace*) and K^+ exchange modes (*gray trace*; 140 mM K^+ or Cs^+ on both sides of the membrane). *F*, average relaxation rate constants obtained from fits of data, such as shown in *E* and Figs. 2*D* and 3*B*, to a sum of two exponentials. Data obtained in the Na^+/glutamate exchange mode are shown for comparison. *Error bars*, S.D.

water molecules start penetrating the transporter to form an aqueous cavity leading to the Na1 site and the aspartate residue in position 405 (analogous to Asp-454 in EAAC1; supplemental Fig. 5*B*). Based on this apo-state, a valence for K^+ binding to the Na1 site of +0.09 was calculated, consistent with an aqueous access pathway for a cation. Finally, we analyzed cation binding

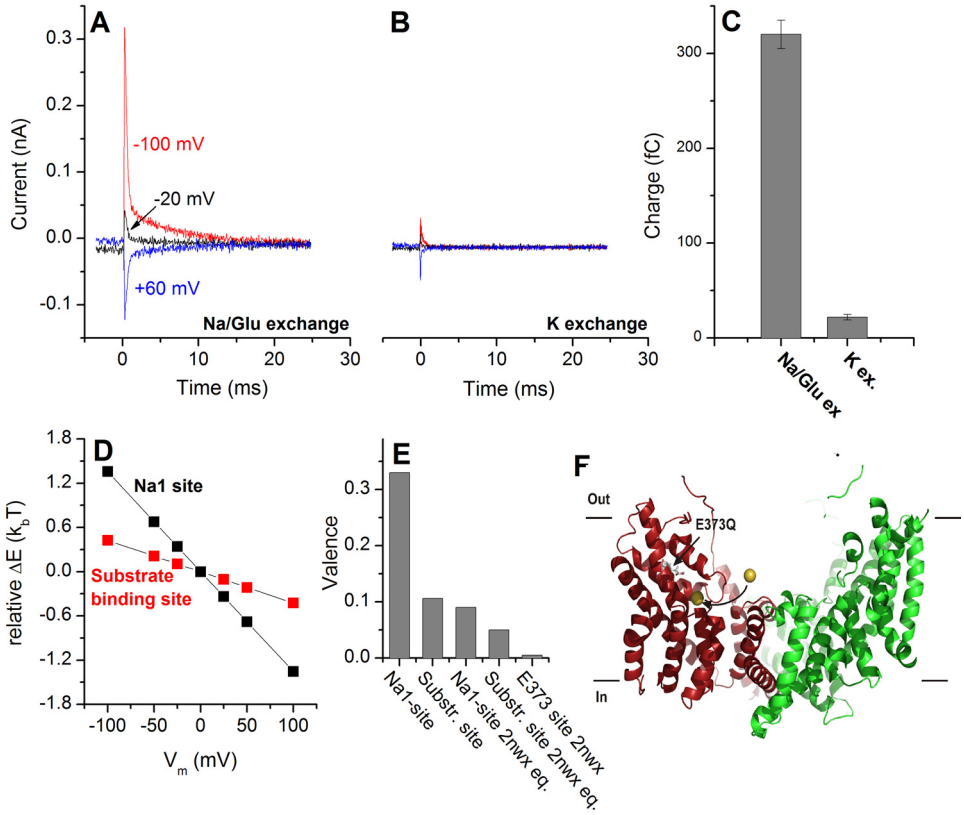

FIGURE 5. **Results from EAAC1(E373Q) reveal that charge movements in the presence of K^+ and Cs^+ are not caused by cation binding.** *A* and *B*, current response after stepping the membrane potential in an EAAC1(E373Q)-expressing cell from −100 to 0 mV in the K^+ exchange (*B*) and Na^+/glutamate exchange modes (*A*); 140 mM K^+ or 140 mM Na^+, 10 mM glutamate on both sides of the membrane. *C*, charge moved in experiments *A* and *B* at −100 mV from an average of $n = 5$ cells. *D*, PB computations of the valence of K^+ binding to EAAC1(WT), as illustrated in *F*. *E*, computed valence for binding of K^+ to several different potential binding sites (EAAC1(WT)). *F*, structural model used for the PB calculations of extracellular K^+ binding to the hypothetical binding site near the Glu-373 side chain. The *arrow* indicates the binding event, and the *yellow sphere* represents the K^+ ion before and after binding. *Error bars*, S.D.

to a potential binding site at position Glu-373 ($z = +0.005$; Fig. 5*E*). Taken together, our experimental and computational results suggest that the extent of voltage dependence of extracellular K^+ binding is small.

Direct Evidence for a Charge Compensation Mechanism—The results from voltage jump analysis do not answer questions about the sign of the charge movement (*i.e.* is positive or negative charge moving within the membrane electric field?). To answer this question, we performed a single turnover K^+ exchange experiment (Fig. 6). Here, K^+ was initially only present on the intracellular side, ensuring an outward facing K^+ binding site. Subsequently, K^+ was rapidly applied to the extracellular side. As expected, if rearrangement of the binding site is associated with negative charge movement, application of 140 mM K^+ to the extracellular side was followed by a transient outward current (Fig. 6*A*, *left*). To test whether the cell functionally expressed glutamate transporters, 1 mM glutamate was rapidly applied to the extracellular side, showing the well characterized, rapidly decaying inward transient current followed by a steady-state component (Fig. 6*B*), demonstrating that the solution exchange procedure is fast enough to detect transient currents. The decay rate of the transient currents is governed by the time resolution of the solution exchange system (~50 ms). Therefore, no quantitative rate information can be obtained in this experiment. However, the experiment directly demonstrates net negative charge of the K^+-loaded transporter, because inward movement of positive charge would be associated with inward transient current. No inward currents were detected in any of the 12 cells observed.

The following control experiments were performed. 1) TBOA virtually abolished the current (Fig. 6*A*, *middle*). 2) The K^+-induced response was absent in control cells (Fig. 6*D*). 3) The application of Cs^+ resulted in much smaller amplitude of the transient current, due to the lower relocation rate of the Cs^+-bound *versus* the K^+-bound transporter (Fig. 6*C*). 4) The charge moved in response to K^+ application is proportional to expression levels (supplemental Fig. 6). 5) Transient outward current precedes steady-state reverse transport current when K^+ is applied to the extracellular side under reverse transport conditions (supplemental Fig. 7, *A–C*). When glutamate was applied to the same cell, inward transient current, but no steady-state component, was observed (supplemental Fig. 7*D*). Together, these control experiments show that the outward charge movement is specifically caused by the glutamate transporter.

Upon removal of K^+, formation of a transient inward current would be expected, if the charge movement is capacitive. This was seen in some but not all cells. The non-consistent nature of observable inward current is most likely caused by difficulties in removing ions rapidly through solution exchange.

As shown previously by Wadiche *et al.* (36), transient currents are induced by voltage jumps in the presence of Na^+ but in the absence of transporter turnover. To test the direction of

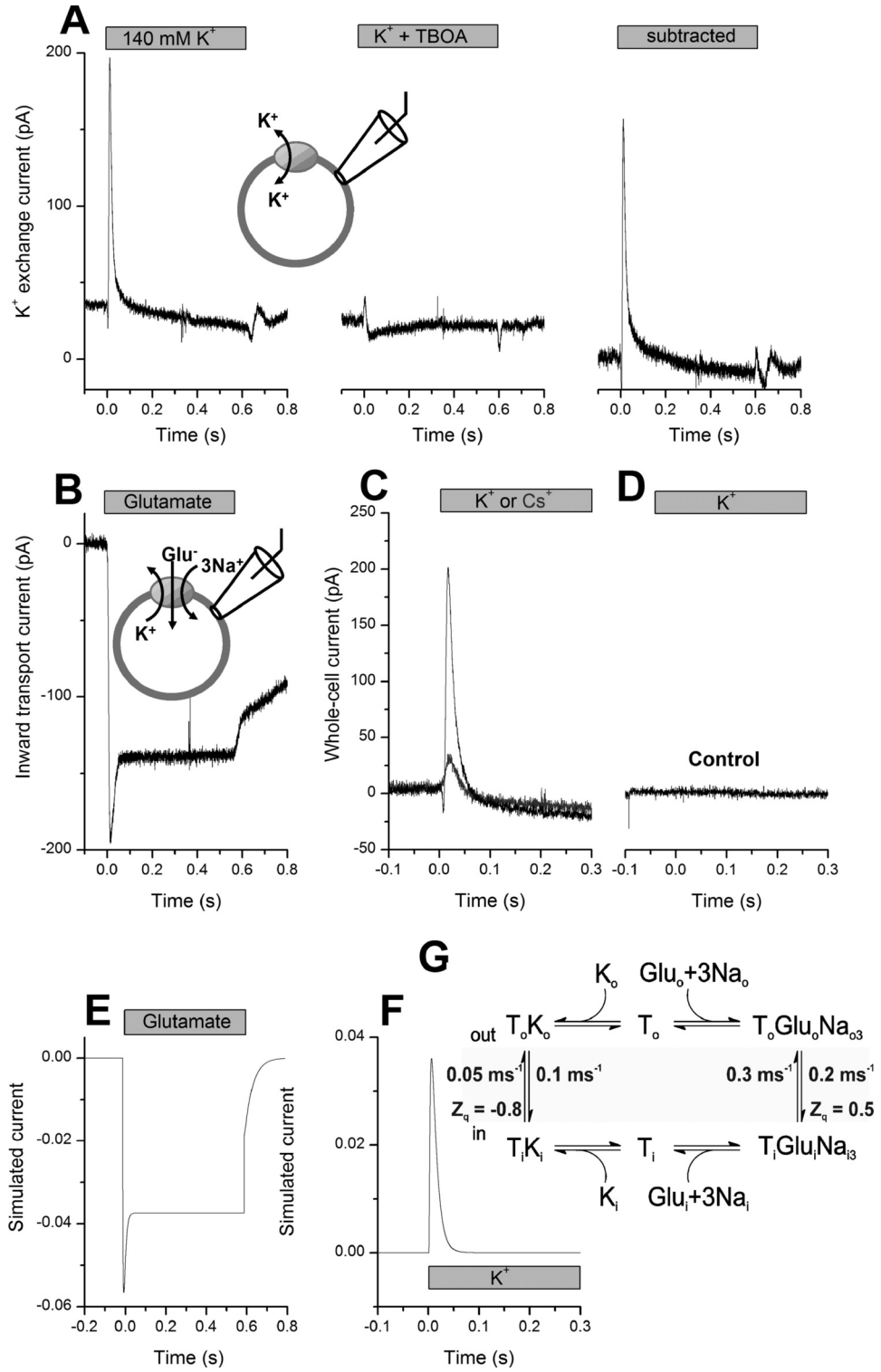

FIGURE 6. **Single turnover K^+ exchange is associated with the movement of negative charge.** *A*, K^+ exchange currents in an EAAC1-expressing cell induced by rapid extracellular solution exchange from NMG^+ to K^+. The intracellular solution contained 120 mM KMes. The middle trace was recorded in the presence of 200 μM TBOA (+ 5 mM Na^+ to promote TBOA binding). The *right*, *subtracted trace* represents the TBOA-sensitive component of the current, which is specific for EAAC1. *B*, rapid application of 1 mM glutamate to the same cell in the presence of 140 mM Na^+ induces inward transport current. *C*, comparison of currents elicited by application of K^+ (*black trace*) or Cs^+ (*gray trace* with lower peak amplitude, 140 mM) EAAC1. *D*, response to K^+ in a non-transfected cell. *A–D* were all recorded at 0 mV. *E* and *F*, simulated current responses in forward transport mode (*E*) and K^+-K^+ exchange mode (*F*) according to the kinetic scheme shown in *G*. Conditions of the simulation were chosen to match the experiments in *B* and *C*. The solution exchange time was 50 ms.

Na^+-induced charge movement, we rapidly applied 140 mM Na^+ to the extracellular side of EAAC1. As shown in supplemental Fig. 8, a transient inward current was observed ($n = 3$ cells). This result is consistent with previous models on electrogenic Na^+ effects (36), showing differential and opposite effects of K^+ and Na^+ interaction with the transporter.

To test the predictions of the single turnover K^+ exchange experiments, we performed numerical simulations according to the kinetic scheme shown in Fig. 6*G*. As shown in Fig. 6*E*, the experimentally observed transient and steady-state inward current induced by glutamate application is well represented by these simulations. Using a valence of −0.8 for the K^+ relocation step, the K^+-induced current can also be reproduced well by the simulations (Fig. 6*F*).

DISCUSSION

The most important conclusion from this work is that transport of glutamate and the co-transported Na^+ ions is based on a charge compensation mechanism, in which intrinsic negative charge of the transporter binding site partially compensates for the three positive charges of the bound cations/substrate in the fully loaded transporter in the translocation step, and overcompensates for the single positive charge of the bound K^+ ion in the relocation step of the empty transporter. Computationally estimated valences of the transporter in various states are in excellent agreement with this conclusion, independent of the protonation state of the conserved amino acid side chain aspartate 454, which is at present ambiguous. In contrast, extracellular K^+ binding is most likely electrically silent because extracellular water penetrates the cation permeation channel in the apo-state of the transporter. At present, our results do not allow us to draw conclusions about the electrogenic nature of intracellular cation binding, although it has been previously suggested that intracellular Na^+ binding and/or conformational changes associated with it cause transmembrane charge movement (22).

Structure function relationship studies on transport systems have focused on ionizable amino acid residues in transmembrane domains with potential negative charge (37), including several reports on glutamate transporters (14, 16, 35). In reports from the Wright laboratory, it was proposed that the sodium-glucose transporter, SGLT1, contains negative charge in its sodium binding site(s), counterbalancing the two positive charges of the co-transported Na^+ ions (38). Similar mechanisms were proposed for the Na^+/phosphate transporter (39). For SGLT1, evidence was based on the fact that the Na^+/glucose translocation step(s) are associated with little charge movement and that voltage jumps applied to the empty transporter result in transient currents, which are sensitive to the SGLT1 inhibitor phlorizin. Although such voltage jump experiments, similar to the ones performed here, prove that the empty transporter is charged, they do not provide evidence on the sign of the charge. To demonstrate this point, we have performed simulations of concentration jumps and voltage jumps (supplemental Fig. 9). Whereas the [K^+] jump (single turnover) experiment allows a clear differentiation between inward and outward charge movement in the presence of positive or negative charge of the transport domain (supplemental Fig. 9, *A* and *C*), the voltage jump experiment shows only minor differences in the kinetics of the transient current signals, but, as expected, the sign of the current is the same in both cases (supplemental Fig. 9, *B* and *D*). Thus, when analysis is based on voltage jump data only, conclusions about the sign of the charge of the binding sites can only be obtained by indirect kinetic modeling or site-directed mutagenesis of charged residues. The glutamate transporter, therefore, represents a valuable model system because, in contrast to many other secondary active transporters, relocation of the empty transporter is not spontaneous but rather triggered by K^+ binding (17). This functional property allowed us to perform the single turnover K^+ exchange experiments shown in Fig. 5, providing direct proof of negative charge of the K^+-loaded transport domain.

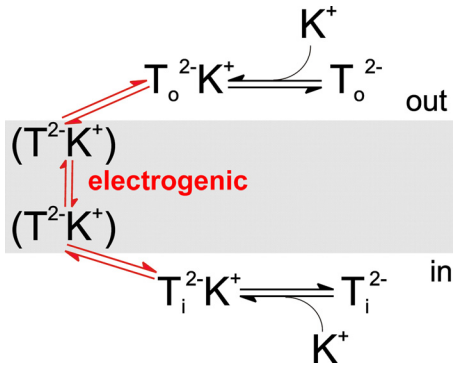

FIGURE 7. **A charge compensation mechanism for K^+ countertransport accounts for the experimental and computational results.** The *red arrows* indicate potentially electrogenic reactions. The *black arrows* indicate electrically silent processes. *T*, is the transporter, with the index *i* indicating inward facing conformation and *o* indicating outward facing conformation.

A noteworthy result from voltage jump analysis is that the relaxation of the transient current is biphasic (supplemental Fig. 2), suggesting that the underlying molecular processes consist of at least two steps. The rate of decay of the slow step is consistent with rate constants previously estimated for the relocation step (10). Furthermore, the apparent valence associated with this charge movement is consistent with the valence of the inward facing to outward facing transition computed using the PB formalism. Therefore, we propose that the slow component of the charge movement is caused by the major conformational reorientation of the transport domain within the membrane (see Fig. 6 for a proposed kinetic mechanism). The relaxation of the slow phase is slower than the relaxation of transient currents in the glutamate/Na^+ homoexchange mode (Fig. 4*F*). This result provides additional evidence that the K^+-induced relocation reaction is rate-limiting for the overall transport cycle in the forward direction (10). The Cs^+ substitution experiments are also consistent with this proposal. Although we cannot directly assign the fast relaxation phase of the transient current to a distinct process in the transport cycle, it can be speculated that it is caused by relaxation of the opening/closing equilibrium of either the internal or the external gate of the transport domain (Fig. 6). Although the gate-opening process is less defined for the internal gate, both structural and molecular dynamics simulation evidence indicates that the external gate is open in the apo-form of the transporter (6, 7). Therefore, it is likely that this gate has to close first in the K^+-bound state, before the transport domain can move within the membrane. In contrast to the electrogenicity of these structural changes, our molecular dynamics simulations and experiments with the E373Q mutant transporter suggest that the K^+ binding process is electrically almost silent. Our results are summarized and illustrated in a kinetic mechanism for K^+-induced relocation shown in Fig. 7. In this mechanism, electroneutral binding of

K^+ to the extra- or intracellular binding sites is followed by potentially electrogenic closure of the reentrant loops, with subsequent electrogenic movement of the negatively charged transport domain within the membrane. It should be noted that the electrical properties of the intracellular binding/gate closure reactions are speculative at this point.

Charge compensation mechanisms, such as the one postulated here, may be a general feature of ion-coupled transporters. This would suggest that the charge of transported cations must be at least partially compensated for to allow efficient ion translocation, which otherwise would have to overcome large electrostatic barriers of inserting a significant amount of charge into the low dielectric environment of the membrane. For example, the Born energy for inserting one Na^+ ion from water into the low dielectric membrane ($\epsilon = 2$) is 350 kJ/mol. Viewed as an activation energy, such high values are prohibitive for transport, considering that the translocation steps of the glutamate transporter have activation energies no higher than 110 kJ/mol (20). Therefore, it can be hypothesized that Na^+-coupled transporters not only require compensation of the charge of the Na^+ ion but also need to fine tune charge balance of the charge-translocating and -relocating steps (*e.g.* by countertransporting K^+ in the case of the EAATs) to avoid paying this electrostatic cost. In addition to charge compensation, the glutamate transporters employ two other strategies to minimize electrostatic barriers. 1) The electric field of the membrane is defocused (Fig. 2*E*). This defocusing reduces the voltage dependence of individual steps. 2) The charge movement is distributed over many individual kinetic steps in the transport cycle, as indicated in the mechanisms shown in Fig. 6. Therefore, each individual step has less voltage dependence and a reduced potential to be inhibited by unfavorable transmembrane potentials. Together, these three mechanisms may lead to a relatively shallow voltage dependence of the transport rate, which is found for the glutamate transporter, as well as for many other secondary active transport proteins, for which detailed electrophysiological data are available (a large list of studied systems includes Refs. 10 and 38–40). Reducing the voltage dependence of substrate transport is particularly important for the glutamate transporter because of the large number of positively charged cotransported ions (three Na^+ and one H^+ (41)). If these charges were transported across the membrane in a single step, transport would be strongly inhibited upon depolarization.

In conclusion, our results provide direct evidence for a charge compensation mechanism of the glutamate transporters, with negative charge of the transport domain overcompensating for the single positive charge of the countertransported potassium ion but only partially compensating for the three positive charges of translocated $3Na^+/H^+$/glutamate$^-$. Together with defocusing of the membrane electric field and distribution of charge movement over many weakly electrogenic steps in the transport cycle, glutamate transporters and possibly other Na^+-coupled secondary active transporters employ this mechanism to prevent paying a large electrostatic energetic penalty for movement of a substantial number of charges through the low dielectric environment of the membrane.

Acknowledgments—We thank K. Callenberg for valuable help with the APBSmem Java routine and H. Fiumera and B. Kanner for helpful discussions and suggestions regarding the K^+ exchange experiments.

REFERENCES

1. Crisman, T. J., Qu, S., Kanner, B. I., and Forrest, L. R. (2009) Inward facing conformation of glutamate transporters as revealed by their inverted topology structural repeats. *Proc. Natl. Acad. Sci. U.S.A.* **106,** 20752–20757
2. Reyes, N., Ginter, C., and Boudker, O. (2009) Transport mechanism of a bacterial homologue of glutamate transporters. *Nature* **462,** 880–885
3. Kaback, H. R., Dunten, R., Frillingos, S., Venkatesan, P., Kwaw, I., Zhang, W., and Ermolova, N. (2007) Site-directed alkylation and the alternating access model for LacY. *Proc. Natl. Acad. Sci. U.S.A.* **104,** 491–494
4. Jardetzky, O. (1966) Simple allosteric model for membrane pumps. *Nature* **211,** 969–970
5. Yernool, D., Boudker, O., Jin, Y., and Gouaux, E. (2004) Structure of a glutamate transporter homologue from *Pyrococcus horikoshii*. *Nature* **431,** 811–818
6. Huang, Z., and Tajkhorshid, E. (2008) Dynamics of the extracellular gate and ion substrate coupling in the glutamate transporter. *Biophys. J.* **95,** 2292–2300
7. Shrivastava, I. H., Jiang, J., Amara, S. G., and Bahar, I. (2008) Time-resolved mechanism of extracellular gate opening and substrate binding in a glutamate transporter. *J. Biol. Chem.* **283,** 28680–28690
8. Boudker, O., Ryan, R. M., Yernool, D., Shimamoto, K., and Gouaux, E. (2007) Coupling substrate and ion binding to extracellular gate of a sodium-dependent aspartate transporter. *Nature* **445,** 387–393
9. Jiang, J., Shrivastava, I. H., Watts, S. D., Bahar, I., and Amara, S. G. (2011) Large collective motions regulate the functional properties of glutamate transporter trimers. *Proc. Natl. Acad. Sci. U.S.A.* **108,** 15141–15146
10. Grewer, C., Watzke, N., Wiessner, M., and Rauen, T. (2000) Glutamate translocation of the neuronal glutamate transporter EAAC1 occurs within milliseconds. *Proc. Natl. Acad. Sci. U.S.A.* **97,** 9706–9711
11. Larsson, H. P., Tzingounis, A. V., Koch, H. P., and Kavanaugh, M. P. (2004) Fluorometric measurements of conformational changes in glutamate transporters. *Proc. Natl. Acad. Sci. U.S.A.* **101,** 3951–3956
12. Watzke, N., Bamberg, E., and Grewer, C. (2001) Early intermediates in the transport cycle of the neuronal excitatory amino acid carrier EAAC1. *J. Gen. Physiol.* **117,** 547–562
13. Rosental, N., Gameiro, A., Grewer, C., and Kanner, B. I. (2011) A conserved aspartate residue located at the extracellular end of the binding pocket controls cation interactions in brain glutamate transporters. *J. Biol. Chem.* **286,** 41381–41390
14. Teichman, S., Qu, S., and Kanner, B. I. (2009) The equivalent of a thallium-binding residue from an archeal homolog controls cation interactions in brain glutamate transporters. *Proc. Natl. Acad. Sci. U.S.A.* **106,** 14297–14302
15. Teichman, S., and Kanner, B. I. (2007) Aspartate 444 is essential for productive substrate interactions in a neuronal glutamate transporter. *J. Gen. Physiol.* **129,** 527–539
16. Tao, Z., Zhang, Z., and Grewer, C. (2006) Neutralization of the aspartic acid residue Asp-367, but not Asp-454, inhibits binding of Na^+ to the glutamate-free form and cycling of the glutamate transporter EAAC1. *J. Biol. Chem.* **281,** 10263–10272
17. Kanner, B. I., and Bendahan, A. (1982) Binding order of substrates to the sodium and potassium ion-coupled L-glutamic acid transporter from rat brain. *Biochemistry* **21,** 6327–6330
18. Wadiche, J. I., and Kavanaugh, M. P. (1998) Macroscopic and microscopic properties of a cloned glutamate transporter/chloride channel. *J. Neurosci.* **18,** 7650–7661
19. Otis, T. S., and Kavanaugh, M. P. (2000) Isolation of current components and partial reaction cycles in the glial glutamate transporter EAAT2. *J. Neurosci.* **20,** 2749–2757
20. Mim, C., Tao, Z., and Grewer, C. (2007) Two conformational changes are associated with glutamate translocation by the glutamate transporter EAAC1. *Biochemistry* **46,** 9007–9018

21. Shimamoto, K., Lebrun, B., Yasuda-Kamatani, Y., Sakaitani, M., Shigeri, Y., Yumoto, N., and Nakajima, T. (1998) DL-threo-β-benzyloxyaspartate, a potent blocker of excitatory amino acid transporters. *Mol. Pharmacol.* **53,** 195–201
22. Zhang, Z., Tao, Z., Gameiro, A., Barcelona, S., Braams, S., Rauen, T., and Grewer, C. (2007) Transport direction determines the kinetics of substrate transport by the glutamate transporter EAAC1. *Proc. Natl. Acad. Sci. U.S.A.* **104,** 18025–18030
23. Baker, N. A., Sept, D., Joseph, S., Holst, M. J., and McCammon, J. A. (2001) Electrostatics of nanosystems. Application to microtubules and the ribosome. *Proc. Natl. Acad. Sci. U.S.A.* **98,** 10037–10041
24. Callenberg, K. M., Choudhary, O. P., de Forest, G. L., Gohara, D. W., Baker, N. A., and Grabe, M. (2010) APBSmem. A graphical interface for electrostatic calculations at the membrane. *PLoS One* **5,** e12722
25. Roux, B. (1997) Influence of the membrane potential on the free energy of an intrinsic protein. *Biophys. J.* **73,** 2980–2989
26. Silva, J. R., Pan, H., Wu, D., Nekouzadeh, A., Decker, K. F., Cui, J., Baker, N. A., Sept, D., and Rudy, Y. (2009) A multiscale model linking ion channel molecular dynamics and electrostatics to the cardiac action potential. *Proc. Natl. Acad. Sci. U.S.A.* **106,** 11102–11106
27. Choudhary, O. P., Ujwal, R., Kowallis, W., Coalson, R., Abramson, J., and Grabe, M. (2010) The electrostatics of VDAC. Implications for selectivity and gating. *J. Mol. Biol.* **396,** 580–592
28. Grewer, C., Balani, P., Weidenfeller, C., Bartusel, T., Tao, Z., and Rauen, T. (2005) Individual subunits of the glutamate transporter EAAC1 homotrimer function independently of each other. *Biochemistry* **44,** 11913–11923
29. Holley, D. C., and Kavanaugh, M. P. (2009) Interactions of alkali cations with glutamate transporters. *Philos. Trans. R. Soc. Lond. B Biol. Sci.* **364,** 155–161
30. Grewer, C., Watzke, N., Rauen, T., and Bicho, A. (2003) Is the glutamate residue Glu-373 the proton acceptor of the excitatory amino acid carrier 1? *J. Biol. Chem.* **278,** 2585–2592
31. Huang, Z., and Tajkhorshid, E. (2010) Identification of the third Na^+ site and the sequence of extracellular binding events in the glutamate transporter. *Biophys. J.* **99,** 1416–1425
32. Barbour, B., Brew, H., and Attwell, D. (1991) Electrogenic uptake of glutamate and aspartate into glial cells isolated from the salamander (Ambystoma) retina. *J. Physiol.* **436,** 169–193
33. Bergles, D. E., Tzingounis, A. V., and Jahr, C. E. (2002) Comparison of coupled and uncoupled currents during glutamate uptake by GLT-1 transporters. *J. Neurosci.* **22,** 10153–10162
34. Auger, C., and Attwell, D. (2000) Fast removal of synaptic glutamate by postsynaptic transporters. *Neuron* **28,** 547–558
35. Pines, G., Zhang, Y., and Kanner, B. I. (1995) Glutamate 404 is involved in the substrate discrimination of GLT-1, a ($Na^+ + K^+$)-coupled glutamate transporter from rat brain. *J. Biol. Chem.* **270,** 17093–17097
36. Wadiche, J. I., Arriza, J. L., Amara, S. G., and Kavanaugh, M. P. (1995) Kinetics of a human glutamate transporter. *Neuron* **14,** 1019–1027
37. Díez-Sampedro, A., Loo, D. D., Wright, E. M., Zampighi, G. A., and Hirayama, B. A. (2004) Coupled sodium/glucose cotransport by SGLT1 requires a negative charge at position 454. *Biochemistry* **43,** 13175–13184
38. Loo, D. D., Hazama, A., Supplisson, S., Turk, E., and Wright, E. M. (1993) Relaxation kinetics of the Na^+/glucose cotransporter. *Proc. Natl. Acad. Sci. U.S.A.* **90,** 5767–5771
39. Forster, I. C., Köhler, K., Biber, J., and Murer, H. (2002) Forging the link between structure and function of electrogenic cotransporters. The renal type IIa Na^+/P_i cotransporter as a case study. *Prog. Biophys. Mol. Biol.* **80,** 69–108
40. Erreger, K., Grewer, C., Javitch, J. A., and Galli, A. (2008) Currents in response to rapid concentration jumps of amphetamine uncover novel aspects of human dopamine transporter function. *J. Neurosci.* **28,** 976–989
41. Zerangue, N., and Kavanaugh, M. P. (1996) Flux coupling in a neuronal glutamate transporter. *Nature* **383,** 634–637